

Research Article

Analysis and Design of Short FRP-Confined Concrete-Encased Arbitrarily Shaped Steel Columns under Biaxial Loading

Wei He,^{1,2} Bing Fu ,^{3,4} and Feng-Chen An⁵

¹School of Water Conservancy and Environment, Zhengzhou University, Zhengzhou, Henan Province, China

²Zhengzhou Metro Co. Ltd., Zhengzhou, Henan Province, China

³School of Civil and Transportation Engineering, Guangdong University of Technology, Guangzhou, Guangdong Province, China

⁴Department of Civil and Environmental Engineering, The Hong Kong Polytechnic University, Hung Hom, Hong Kong

⁵College of Petroleum Engineering, China University of Petroleum, Beijing, China

Correspondence should be addressed to Bing Fu; cefubing@gdut.edu.cn

Received 25 June 2018; Revised 26 September 2018; Accepted 30 September 2018; Published 25 November 2018

Academic Editor: Mehdi Salami-Kalajahi

Copyright © 2018 Wei He et al. This is an open access article distributed under the Creative Commons Attribution License, which permits unrestricted use, distribution, and reproduction in any medium, provided the original work is properly cited.

The FRP-confined concrete-encased steel column is a new form of hybrid column, which integrates advantages of all the constituent materials. Its structural performance, including load carrying capacity, ductility, and corrosion resistance, has been demonstrated to be excellent by limited experimental investigation. Currently, no systematic procedure, particularly for that with reinforced structural steel of arbitrary shapes, has been proposed for the sectional analysis and design for such novel hybrid columns under biaxial loading. The present paper aims at filling this research gap by proposing an approach for the rapid section analysis and providing rationale basis for FRP-confined concrete-encased arbitrarily shaped steel columns. A robust iterative scheme has been used with a traditional so-called fiber element method. The presented numerical examples demonstrated the validity and accuracy of the proposed approach.

1. Introduction

Lateral confinement leads to the compressed concrete under multiaxial compression and results in enhancements in both ductility and strength of the compressed concrete [1]. Such a feature is highly preferable for design and constructing columns in a region of high seismic risk, where adequate ductility of columns is necessary to ensure high moment redistribution capacity of structures and avoid collapse of structures due to the shaking from large earthquakes [2]. In conventional reinforced concrete structures, the lateral confinement to the compressed concrete is mainly provided by the transverse steel reinforcement in the form of either spirals or hoops. Concrete-filled steel tubular columns, which have been widely used in high-rise buildings, bridges, etc., are also utilizing the increased strength and deformability of confined concrete to achieve a high structural performance [3, 4]. In such a composite column, an outer steel tube is used to replace longitudinal and transverse steel reinforcements in

conventional reinforced concrete columns and to provide continuous confinement to concrete infilled. However, such a concrete-filled steel tubular column, especially in a harsh environment, is susceptible to severe corrosion problem due to the direct exposure of the outer steel tube to ambient environment.

Fiber reinforced polymer (FRP) composites in the form of wraps or jackets have been widely used to serve as a confining device for seismic retrofit of existing RC columns [5, 6]. Its wide application is mainly attributed to the superior properties of FRP composites, such as high strength-to-weight ratio and excellent corrosion resistance. Recently, combining FRP composites with traditional construction materials (e.g., steel and concrete) has gained increasing research attention to form a hybrid column to achieve high structural performance by integrating advantages of the constituent materials. A successful example is the hybrid FRP-concrete double-skin tubular columns (DSTCs), which was proposed by Teng et al. [7] and then

received a great deal of follow-on research (e.g., [8–13]). A DSTC consists of an FRP outer tube, a steel inner tube, and a layer of concrete sandwiched between them [7]. The FRP tube offers mechanical resistance primarily in the hoop direction to confine the concrete and to enhance the shear resistance of the member; the steel tube provides the main longitudinal reinforcement and prevents the concrete from inward spalling and the steel tube from outward local buckling deformations. Optimal use of FRP, steel, and concrete in the manner of DSTC therefore makes it an economical and corrosion-resistant column form.

Another successful example that integrates advantages of all the constituent materials into a hybrid column is the FRP-confined concrete-encased steel composite columns (FCSCs), which was first proposed by Liu et al. [14] for retrofit of existing steel columns. In their study, five notched steel columns to simulate the corroded section were encased using FRP-confined concrete to enhance its load carrying capacity, and tests results demonstrated the feasibility of such a retrofit technique. Karimi and his coauthors [4, 15, 16] then introduced the FCSCs for the new construction of a column and conducted a systematic experimental study on the compressive behavior of both short and slender FCSCs. Recently, Yu et al. [17] presented a combined experimental and theoretical study on the behavior of FCSCs under concentric and eccentric compression and revealed that two flanges of H-shaped steel could provide additional confinement to infilled concrete thus enhancing the ductility and load carrying of the composite columns. In order to further enhance the confinement efficiency for FRP-confined concrete-encased steel composite square columns and inspired by Yu et al. [17], Huang and his coauthors [18] innovatively proposed a new form of FCSCs, in which a cross-shaped steel section was used to replace H-shaped (or I-shaped) steel. Their test results demonstrated that despite concrete infill in square section, it was effectively confined by both outer tube and cross-shaped steel and justified the rationales of the proposed new form of composite columns. In some cases, such as corner columns of buildings, irregular cross section or regular cross section placed asymmetrically is often encountered [19]. Despite the fact that the structural performance of FCSCs has been demonstrated by a number of concentric or eccentric compression tests, no approach has been proposed for a rapid section analysis and design of FCSCs with arbitrarily shaped steel and under biaxial loading.

Against the above background, the present paper proposes an approach for the rapid section analysis and provides rationale basis for FRP-confined concrete-encased arbitrarily shaped steel columns. The robust iterative scheme proposed by Chen et al. [19] has been adopted with a traditional so-called fiber element method, where all the constitutive materials were treated as fiber elements avoiding the integration for the stress block of the FRP-confined concrete. The presented numerical examples demonstrated the validity and accuracy of the proposed approach.

2. Methodology

A proper approach is necessary for robust convergence of the exact location of the neutral axis. The iterative procedure proposed by Chen et al. [19] has been adopted herein, in which the iterative quasi-Newton procedure is employed within the Regula-Falsi numerical scheme for the solution of equilibrium equations. In addition, the use of the plastic centroidal axes of the cross section as the reference axes of loading guarantees the convergence of solution in the iterative process. All the constituent materials, including FRP-confined concrete under the combination of axial compression and bending, are treated as fiber elements to avoid the definition of stress block for the FRP-confined concrete, which is difficult to analytically determine. Appropriate constitutive models were used to simulate the mechanical properties of the constituent materials. For instance, strain gradient along the section has been taken into account in the constitutive model of the confined concrete, which is simulated by using a so-called variable confinement stress-strain model proposed in the Chinese code (GB50608-2010).

2.1. Basic Assumptions. The sectional analyses and design in the present paper were conducted based on the following basic assumptions:

- (1) Section plane remains plane after loading; this assumption ensures that the strain at any point of the cross section is proportional to its distance from the neutral axis
- (2) Failure limit state is only defined by the attainment of the strain ϵ_{cu} of the extreme compression fiber; this means no failure mode of steel/steel bar rupture has been considered
- (3) Tensile strength of confined concrete is neglected
- (4) No contribution of FRP tubes to compressive strength of composite columns has been taken directly into account in the section analysis

2.2. Definition of the Reference-Loading Axes. If the usual definition of reference-loading axes (i.e., geometric centroid as its origin) is used, it is possible that the origin of the loading may fall outside the $M_x - M_y$ interaction curve, especially when the axial load is close to the axial load capacity of columns with irregular structural steel under concentric compression [19]. To overcome such divergence difficulty, Chen et al. [19] accepted the plastic centroid of the cross section of columns as the origin of the reference-loading axes. Such definition of the origin of the reference-loading axes ensures α_m , which is the inclination of resultant bending moment resistance and is equal to $\arctan(M_y/M_x)$ and increases monotonically from 0 to 2π with increase of θ_n , orientation of neutral axis from 0 to 2π . In this way, the existence and uniqueness of θ_n and convergence are guaranteed.

For any arbitrary cross section, the definition of the plastic centroid (i.e., the origin of loading-reference axes in this study) was given in (1) and (2):

$$X_{pc} = \frac{X_c A_c f_c / \gamma_c + X_s A_s f_s / \gamma_s + X_r A_r f_r / \gamma_r}{X_c A_c f_c + X_s A_s f_s + X_r A_r f_r}, \quad (1)$$

$$Y_{pc} = \frac{Y_c A_c f_c / \gamma_c + Y_s A_s f_s / \gamma_s + Y_r A_r f_r / \gamma_r}{Y_c A_c f_c + Y_s A_s f_s + Y_r A_r f_r}, \quad (2)$$

in which A_c , A_s , and A_r are areas of concrete, shaped steel, and steel rebars, respectively; γ_c , γ_s , and γ_r are the safety of confined concrete, shaped steel, and steel rebars, respectively; and f_c , f_s , and f_r are the respective characteristic strength of confined concrete, shaped steel, and steel rebars and set to be the ultimate strength of confined concrete, yielding strength of shaped steel and steel rebars, respectively.

2.3. Fiber Element Method Adopted. In the present paper, all the structural components in the composite columns, including the confined concrete, structural steel, and steel bars, have been treated as fiber elements to calculate the stress resultants. This approach avoids the difficulty of the determination of the stress block for confined concrete under bending with/without axial compression. Cross section of any shape has been first meshed to determine the stress resultants of each component. The total resultants of each component can be obtained by a summation over all the fiber elements given by (3), (4), and (5):

$$N_z = \sum_{i=1}^{m_c} \sigma_{ci} A_{ci} + \sum_{j=1}^{m_s} \sigma_{sj} A_{sj} + \sum_{k=1}^{m_r} \sigma_{rk} A_{rk}, \quad (3)$$

$$M_x = - \sum_{i=1}^{m_c} \sigma_{ci} A_{ci} y_{ci} - \sum_{j=1}^{m_s} \sigma_{sj} A_{sj} y_{sj} - \sum_{k=1}^{m_r} \sigma_{rk} A_{rk} y_{rk}, \quad (4)$$

$$M_y = - \sum_{i=1}^{m_c} \sigma_{ci} A_{ci} x_{ci} - \sum_{j=1}^{m_s} \sigma_{sj} A_{sj} x_{sj} - \sum_{k=1}^{m_r} \sigma_{rk} A_{rk} x_{rk}, \quad (5)$$

where N_z , M_x , and M_y are the stress resultants of axial compression, moment over x -axis, and moment over y -axis, respectively; m_c , m_s , and m_r are the numbers of concrete fibers, structural steel fibers, and reinforcing bar fibers, respectively; σ_{ci} , σ_{sj} , and σ_{rk} are the stresses of each concrete fiber, structural steel fiber, and reinforcing bar fiber, respectively; and A_{ci} , A_{sj} , and A_{rk} are areas of respective concrete fiber, structural steel fiber, and reinforcing bar fiber, respectively.

2.4. Modelling of Confined Concrete. The behavior of concrete confined by FRP jacketing has been extensively investigated, and a number of strength models have been developed (e.g., [5, 20–22]). All the strength models, which give the stress-strain relationship explicitly, can be used in the proposed approach; however, a simple and generally accurate model is more preferable for such a design purpose. A stress-strain model of confined

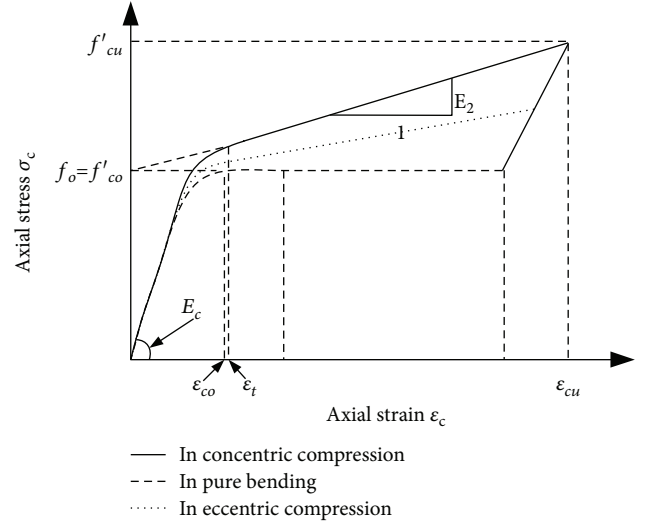


FIGURE 1: Stress-strain models for concrete in FRP-jacketed composite columns.

concrete in the Chinese code (GB50608-2010), which reflects the effect of strain gradient along the section, has therefore been adopted in the present section analysis. In this model, the slope of the second portion of the stress-strain curve (i.e., E_2) is defined as a function of the load eccentricity and equal to be that of the confined model in Lam and Teng [5] for the concrete under the concentric compression (i.e., a zero load eccentricity) and to be zero for the concrete under pure bending (i.e., an infinite load eccentricity).

As shown in Figure 1, the strain-stress relationship of confined subjected to pure bending is formulated by (6) and (7), while that under eccentric compression is given in (8) and (9).

$$\sigma_{cc} = E_1 \epsilon_{cc} - \frac{E_1^2}{4f_c} \epsilon_{cc}^2 \quad \text{for } 0 \leq \epsilon_{cc} \leq \frac{2f_c}{E_1}, \quad (6)$$

$$\sigma_{cc} = f_c \quad \text{for } \frac{2f_c}{E_1} \leq \epsilon_{cc} \leq \epsilon_{cc,ub}, \quad (7)$$

in which σ_{cc} and ϵ_{cc} are the axial stress and axial strain, respectively; $\epsilon_{cc,ub}$ is the design ultimate compressive strain of the concrete subjected to pure bending; E_1 is the elastic modulus of unconfined concrete; and f_c is the design compressive strength of unconfined concrete.

$$\sigma_{cc} = E_1 \epsilon_{cc} - \frac{(E_1 - E_{2,ec})^2}{4f_c} \epsilon_{cc}^2 \quad \text{for } 0 \leq \epsilon_{cc} \leq \epsilon_t, \quad (8)$$

$$\sigma_{cc} = f_c + E_{2,ec} \epsilon_{cc} \quad \text{for } \epsilon_t \leq \epsilon_{cc} \leq \epsilon_{cc,uec}, \quad (9)$$

in which $\epsilon_{cc,uec}$ is the design ultimate compressive strain of the concrete in sections subjected to eccentric compression and $E_{2,ec}$ is the slope of the second linear portion of the

stress-strain curve. Related parameters above are determined by using the following equations:

$$\begin{aligned}\varepsilon_t &= \frac{2f_c}{(E_1 - E_{2,ec})}, \\ E_{2,ec} &= E_2 \frac{d}{d + e_i}, \\ E_2 &= \frac{f'_{cc} - f_c}{\varepsilon_{cu}}, \\ \varepsilon_{cc,uec} &= (\varepsilon_{cc,u} - \varepsilon_{cc,ub}) \frac{d}{d + e_i} + \varepsilon_{cc,ub},\end{aligned}\quad (10)$$

in which E_2 is the slope of the second portion of the stress-strain curves for the FRP-confined concrete under axial compression; f'_{cc} is the ultimate strength of the confined concrete under concentric compression; d is the diameter of the concrete core; e_i is the load eccentricity; and $\varepsilon_{cc,ub}$ is the design ultimate compressive strain of the concrete subjected to pure bending. Such a parameter should be determined from tests and is defined as the smaller value of the design ultimate strains obtained from the axial compression tests on concrete-filled FRP tubes and hollow FRP tubes, respectively. Due to lack of test data, the present manuscript assumes $\varepsilon_{cc,ub}$ be equal to the corresponding ultimate strain of FRP-confined concrete under concentric compression. Such an assumption cannot lead to a significant loss in accuracy and will not adversely affect the main purpose of the present manuscript, which is to validate the proposed approach for the rapid section analysis of FRP-confined concrete-encased arbitrarily shaped steel columns. ε_{cu} , the ultimate strain of FRP-confined concrete under concentric compression, can be determined following [5] as follows:

$$\frac{\varepsilon_{cu}}{\varepsilon_{co}} = 1.75 + 12 \left(\frac{f_{l,a}}{f_c} \right) \left(\frac{\varepsilon_{h,rup}}{\varepsilon_{co}} \right)^{0.45}, \quad (11)$$

in which ε_{cu} and ε_{co} are the ultimate strains of the confined concrete under concentric compression and unconfined concrete, respectively; $\varepsilon_{h,rup}$ is the ultimate hoop strain of the FRP reinforcement; and $f_{l,a}$ is the actual maximum confining pressure given in the following:

$$f_{l,a} = \frac{2E_{FRP}t\varepsilon_{h,rup}}{d}, \quad (12)$$

where E_{FRP} is elastic modulus of the FRP composite.

As revealed by Lam and Teng [23], the ultimate hoop strains of FRP measured in tests on FRP-confined concrete cylinders are substantially below those from flat coupon tensile tests. As a result, a reduction factor for the determination of hoop strains of FRP based on the ultimate rupture strain of FRP from coupon tensile tests should be included, e.g., 0.586 for CFRP and 0.624 for GFRP in the present paper.

2.5. Modelling of Shaped Steel and FRP Tubes. In the sectional analysis, the structural steel and/or steel bars were also

treated as fiber elements with perfectly plastic property and the plane section assumption. The plane section assumption is generally valid, because compression force resisted by the column leads to the expansion of concrete and therefore significant interaction between different constituents. The size of elements should match that of concrete elements. The effect of FRP tubes on structural performance has been taken into account by modifying the constitutive of the confined concrete with the amount of FRP tubes. This means that no axial loading was carried by FRP tubes and no elements in analysis represent the FRP tubes. This makes sense as the fiber of tubes is hoop or predominantly hoop, mainly providing confinement to the concrete core. Neglecting the contribution of FRP tubes to axial load resistance is therefore reasonable and leads to a slightly conservative prediction, which is preferable for a design purpose.

2.6. Iterative Procedure for the Sectional Analysis. For a given composite column, a $M_x - M_y$ interaction curve under a given axial load can be determined by the sectional analysis. The series of such $M_x - M_y$ interaction curves under different axial loads can be utilized to judge whether one composite column satisfies the load carrying requirement. For example, a point representing a design load set (N_{zd}, M_{xd}, M_{yd}) that falls outside the interaction curves means the design column does not satisfy the load carrying requirement; otherwise it is appropriate for use. Detailed iterative procedure for the sectional analysis of a FRP-confined column with structural steel of any shape is given in Figure 2(a). In this iterative procedure, the iterative solution method for parameter d_n is adopted that was presented in Chen et al. [19], and similar approach is used for the eccentricity e .

2.7. Design of Required Dimensions of Hybrid Columns. It is a common task for civil engineers to design the dimensions for a composite column with a given cross section under known loads N_{zd} , M_{xd} , and M_{yd} . In this task, all structural parameters, except the size of structural steel, are specified, and its purpose is to determine the size of structural steel for such a column. The iterative procedure presented in Figure 2(b) is used for this task.

3. Effect of Constitutive Model of Confined Concrete

As mentioned in previous sections, different constitutive models have been proposed by researchers and adopted for the sectional analysis for the composite columns under the combination of axial compression and bending. Good agreement between analytical results and test results on hybrid FRP double-skin composite columns was obtained by [24], where the constitutive models for concrete in pure bending were adopted for analysis. However, such simplification may result in too conservative results, especially for the columns confined by FRPs of a large amount and under eccentric compression with a small eccentricity. In this section, sectional analyses with different constitutive models

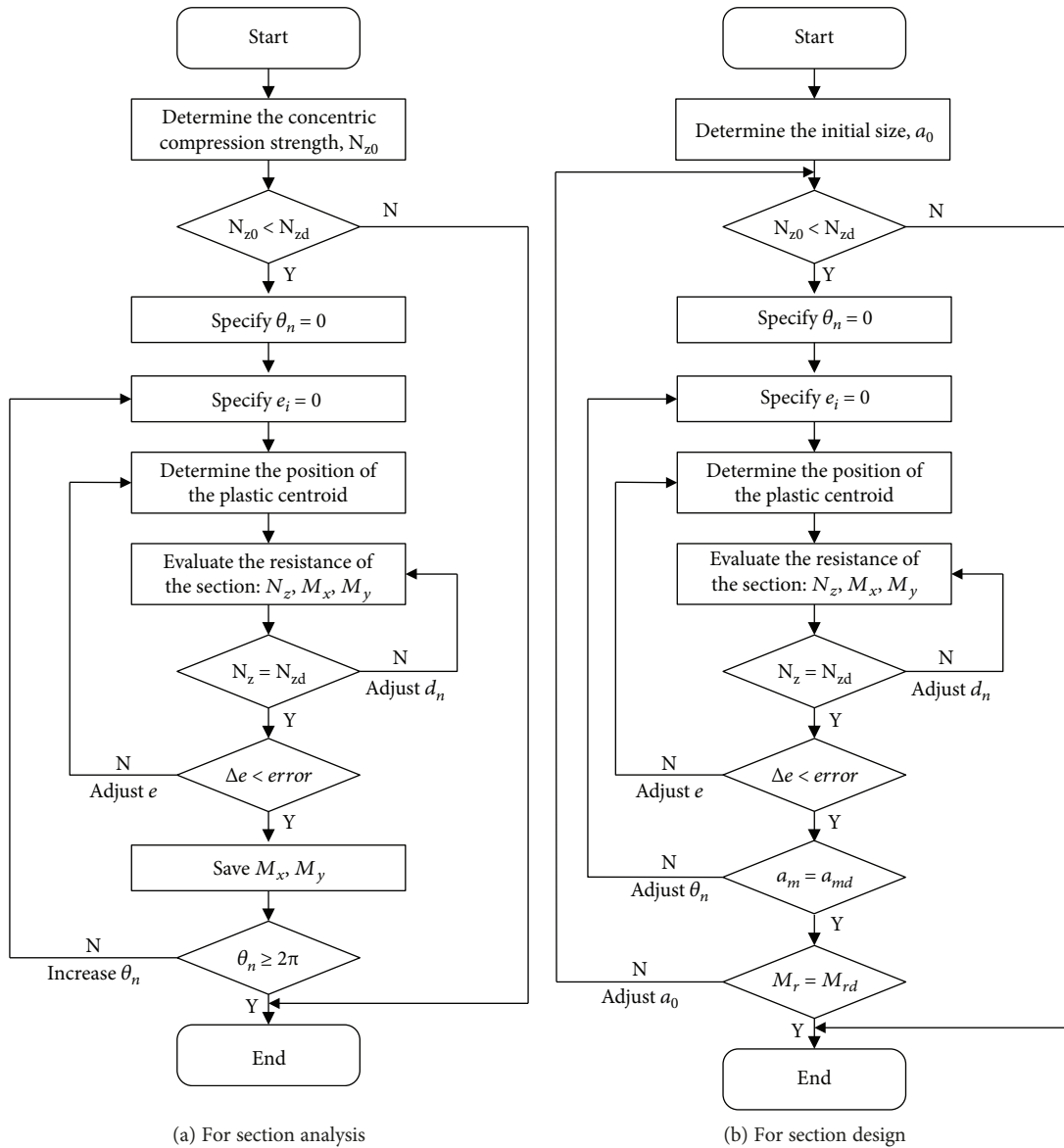


FIGURE 2: Flowcharts for section analysis and design of composite columns under biaxial loading.

for the column have been conducted to investigate the discrepancies induced by different uses of constitutive models for the confined concrete under eccentric compression. Three representative models for confined concrete in Figure 1 were adopted herein for the composite columns under eccentric compression with different eccentricities. It is believed that the sectional analysis with the constitutive models for the confined concrete under pure bending provides the lower limit prediction (denoted as lower limit in following figures), while that from the constitutive model for the confined concrete under axial compression leads to the lower limit prediction (denoted as the lower limit in following figures).

A composite column, which consists of a T-shaped steel, an outer FRP tube, and concrete infilled between them (Figure 3(a)), was analyzed with the mesh given in

Figure 3(b) using the proposed approach. Three different constitutive models illustrated in Figure 1 were used for confined concrete infilled in the section analysis, leading to three curves for each case, respectively, under the axial compression loads of 1500 kN and 2100 kN (Figure 4). The results from the section analysis indicate that bending moments calculated with use of the lower limit model are significantly lower than those from other two models by about 33%, and such differences tend to be more significant in the case with the axial compression load of 2100 kN. However, differences between bending moments calculated using the upper model and middle mode are minor and can be neglected.

Some conclusions drawn from the sectional analysis above are as follows: (1) the discrepancies between the sectional analysis with the upper model and that with the middle model are small and can be neglected if the eccentricity is

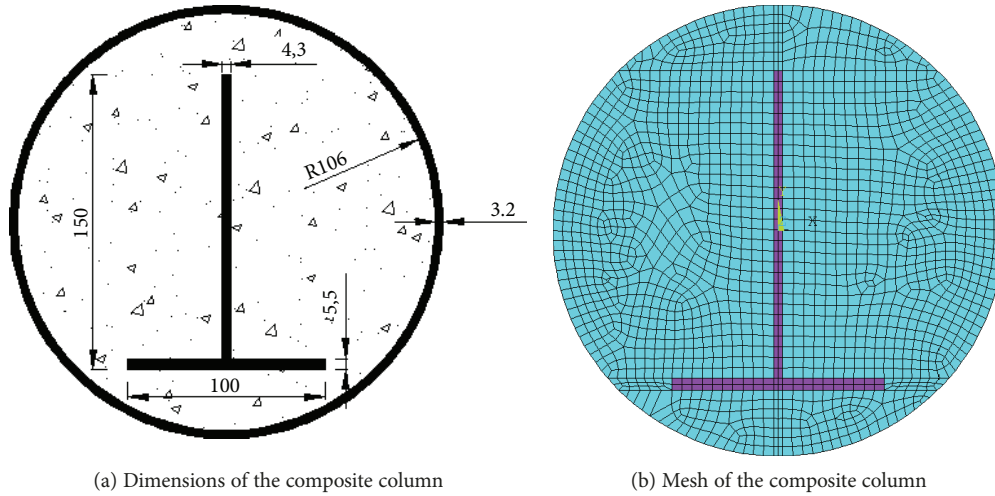


FIGURE 3: Dimensions and mesh of the predefined column; effect of stress-strain models of confined concrete.

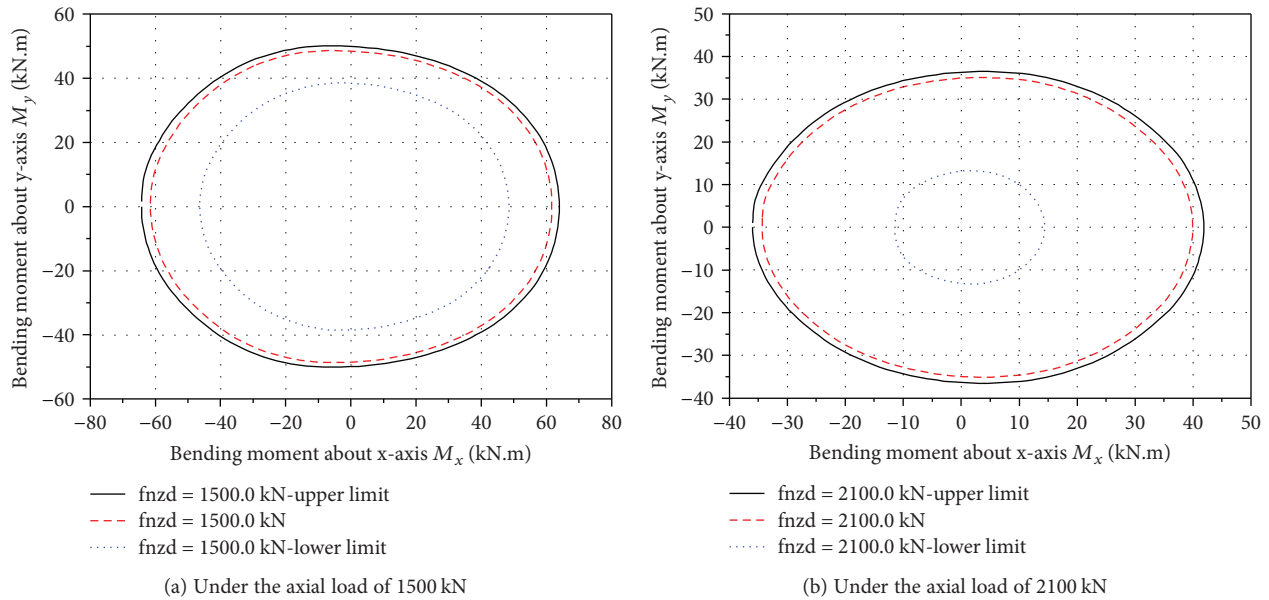


FIGURE 4: $M_x - M_y$ interaction curves of the predefined column; effect of stress-strain models of confined concrete.

small, and (2) the lower model may be too conservative for the sectional analysis of the columns under eccentric compression with small eccentricity and high compression load.

4. Effect of Mesh Schemes

As in all analysis with the fiber element approach, element size plays a significant role in the accuracy and efficiency of the analysis. Coarse mesh for the fiber element may result in inaccuracy in the analysis, while high computational cost may be induced by the refined mesh of the fiber elements. To find an optimal mesh for subsequent calculation, the effect of mesh on the sectional analysis was conducted.

To achieve this aim, four different mesh schemes in Figure 5 were adopted herein (i.e., element sizes of 2 mm, 5 mm, 20 mm, and 40 mm, respectively).

The sectional analysis for the column with four different mesh schemes in Figure 5 was given in Figure 6. The results from the sectional analysis with mesh scheme-2 are almost the same as those from the sectional analysis with mesh scheme-1, and thought to be pretty precise. The results from the mesh scheme-3 are also good with minor discrepancies compared with those from mesh scheme-3. As shown in Figure 6, large discrepancies can be found in the results from the mesh scheme-4 due to the use of coarse fiber elements. It also should be mentioned here that the computational cost of that with mesh scheme-1

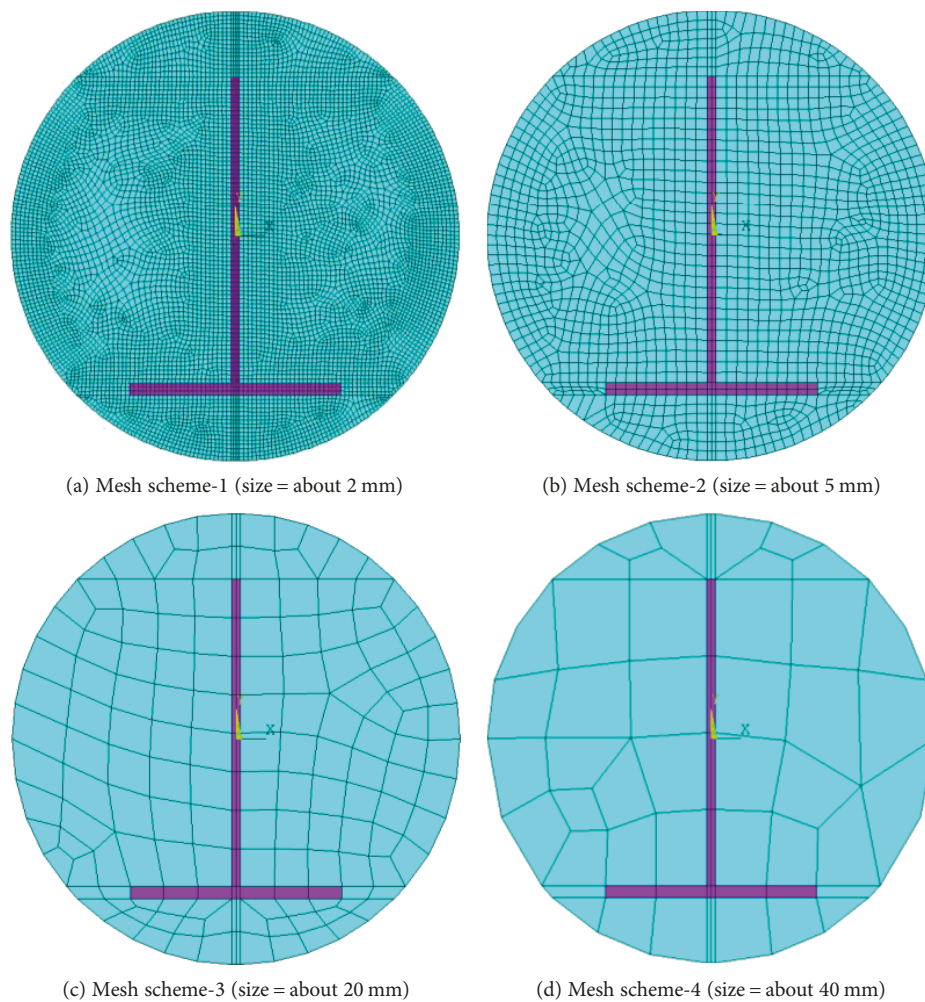


FIGURE 5: Mesh schemes for the predefined column.

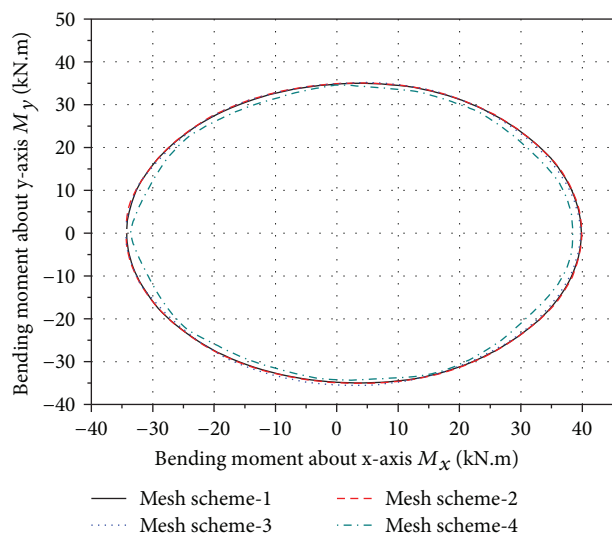


FIGURE 6: $M_x - M_y$ interaction curve with different mesh schemes.

is high. The mesh scheme-2 will be used for the subsequent sectional analysis, which combines the advantage of accuracy and computational cost.

5. Numerical Examples

Several numerical examples, including sectional analysis for a given composite short column, check of the adequacy of predefined cross section, and design of required structural steel, are presented herein to demonstrate the validity and efficiency of the proposed approach.

5.1. Analysis of Designed Cross Section. A FRP-confined concrete-encased I-shaped steel column tested by Karimi et al. [15] is first analyzed in this section. The GFRP tube with fiber orienting in the circumferential direction and its thickness is 3.2 mm. The structural steel is of I-shape and 500 mm long W150 × 14 section. For details of dimension, the readers can refer to Figure 7(a). Mesh of fiber elements was given in Figure 7(b). The $M_x - M_y$ interaction curve (i.e., the isoload contour) of the design cross section (Figure 8) under different axial loads can be easily obtained by the proposed approach. As shown in Figure 8, the resistance along the x -axis is stronger than that along the y -axis, and the x -axis can be taken as the strong axis in design.

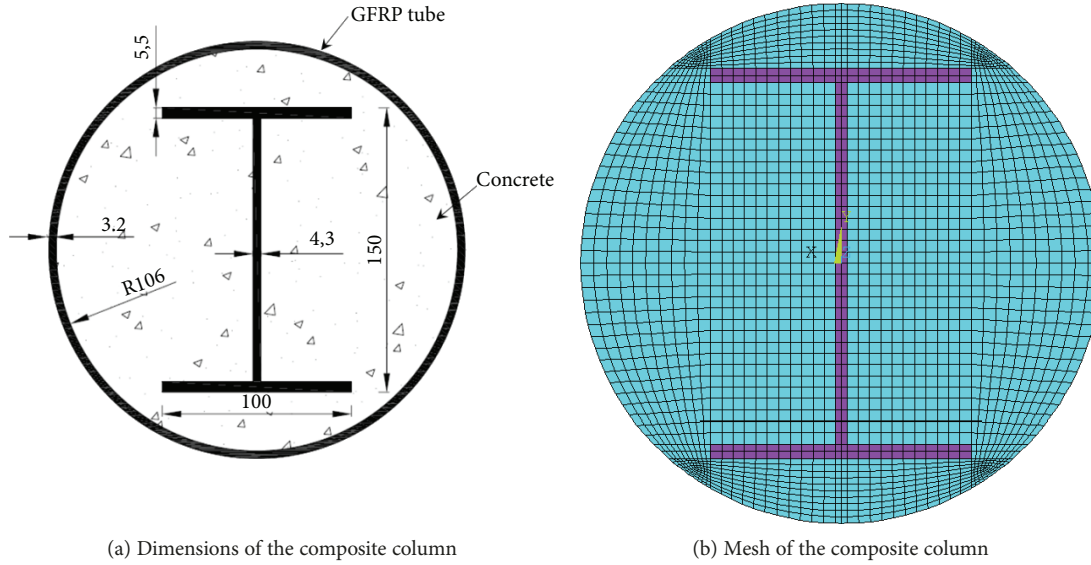


FIGURE 7: Dimensions and mesh of the composite column tested by Karimi et al. [15].

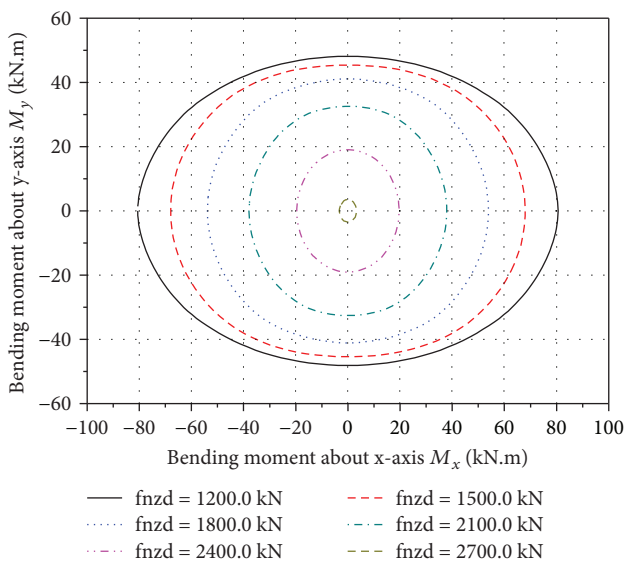


FIGURE 8: $M_x - M_y$ interaction curves of the composite column tested by Karimi et al. [15] under different axial load levels.

To demonstrate the robust ability of the proposed approach for different cross sections, one composite column with more symmetric structural steel was analyzed using this proposed procedure. As shown in Figure 9, a cross-shaped steel was placed in the composite column. As shown in Figure 10, the more symmetric placement of structural steel results in a more symmetric $M_x - M_y$ interaction curve (i.e., the isoload contour); the ultimate resistance along both two axes was almost equal. If no strong axis is required, such placement of structural steel may be preferred for designers.

As mentioned above, the proposed iterative procedure can also be conducted for the columns with structural steel of arbitrary shapes. The following example was used to

demonstrate this ability of the proposed approach. A T-shape structural steel (Figure 3) was used in the composite column; its $M_x - M_y$ interaction curve was obtained using the proposed procedure.

5.2. Checking Adequacy of Predefined Cross Section. Checking the adequacy of predefined cross section is a routine task for structural engineers. For a short FRP-confined concrete-encased arbitrarily shaped steel columns, such a task can be accomplished by comparing the design load with the $M_x - M_y$ interaction curve produced from the proposed section analysis approach. If the load point falls outside the interaction curve, the composite column cannot carry the design load, otherwise indicating the adequacy of the predefined column. For example, the design task is to check whether a composite column with the predefined section in Figure 11 can carry the design load (2200.0 kN, 40.0 kN.m, and 40.0 kN.m). The checking procedure includes (1) spotting the bending moment pair (i.e., 40.0 kN.m, 40 kN.m) in Figure 11, (2) drawing the part of the $M_x - M_y$ interaction curve of 2200.0 kN in the axial load near the design bending moment pair, and (3) checking whether the design bending moment pair falls within the interaction curve or not. It is found herein that this bending moment pair falls outside the interaction curve, indicating the inadequacy of the section and a stronger cross section in need.

5.3. Design of Required Steel Size. The design task is to find a required structural steel size for a composite column to accommodate a specific load set (N_{zd}, M_{xd}, M_{yd}). The iterative procedure in Figure 2(b) can be followed to accomplish this task. For example, dimensions of the composite column, including the type of structural shape, were given in Figure 7. Determine the size of structural steel which can accommodate the load set (2400.0 kN, 71.0 kN.m,

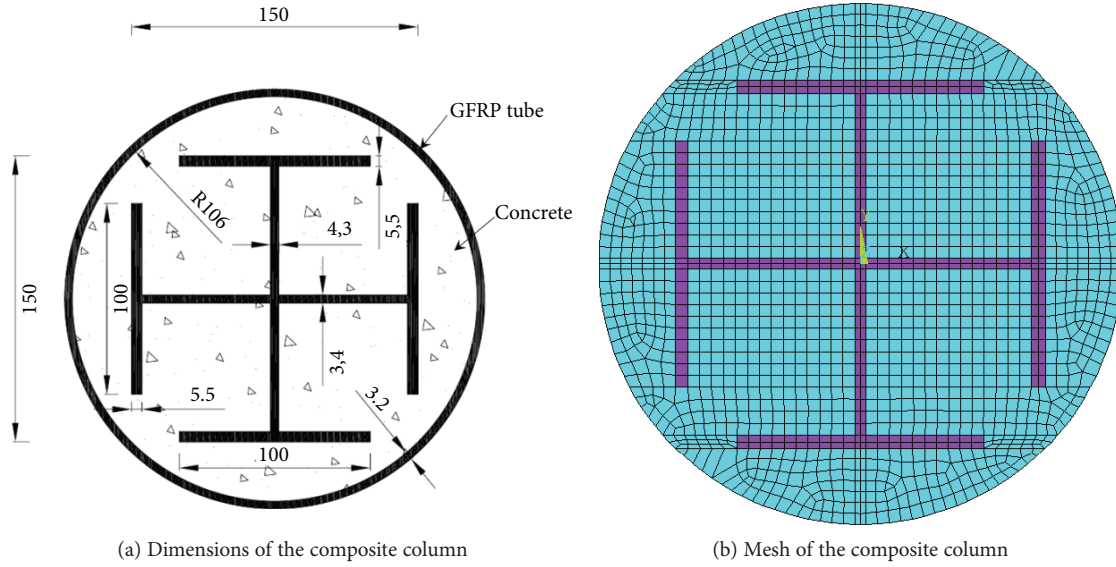


FIGURE 9: Dimensions and mesh of the composite column with a cross-shaped steel.

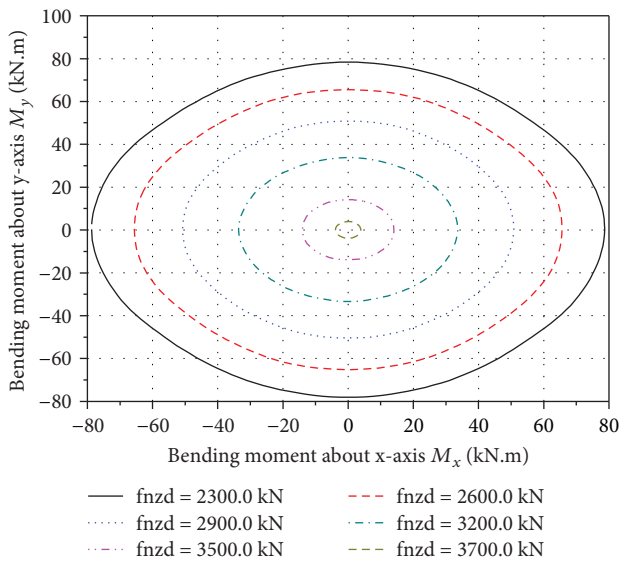


FIGURE 10: $M_x - M_y$ interaction curves of the composite column with a cross-shaped steel under different axial load levels.

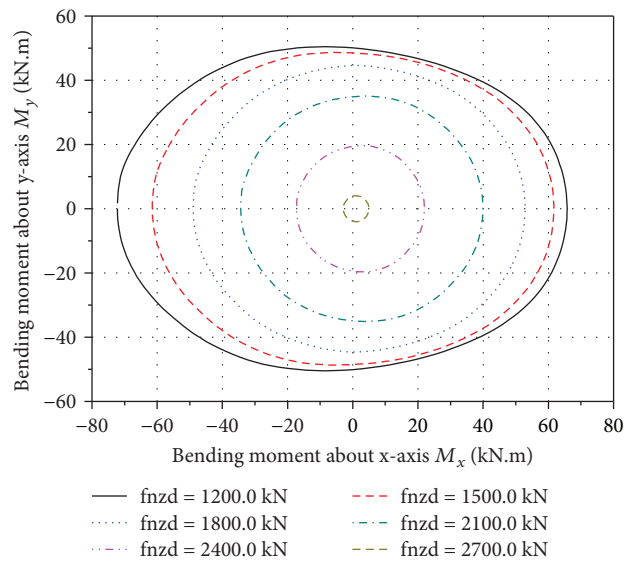


FIGURE 11: $M_x - M_y$ interaction curves of the composite column with a T-shaped steel under different axial load levels.

and -47.9 kN.m). Following the iterative procedure in Figure 2(b), the required size of steel should be 3.316 times that used in Figure 11. In addition, specific dimensions for shaped steel are given in different national codes, so dimensions should also satisfy such requirement.

6. Conclusions

This paper presents an approach for the rapid sectional analysis and design of short FRP-confined concrete-encased arbitrarily shaped steel columns under biaxial loading. A robust iterative scheme has been adopted with a traditional so-called fiber element method, where all the

constituent materials were treated as fiber elements avoiding the integration for the stress block of the FRP-confined concrete. Several numerical examples were presented leading to the conclusions summarized as below:

- (1) Use of the plastic centroid as the origin of reference-loading axes guarantees the convergence in the iterative process. Such a definition of reference-loading axes avoids the possibility that the origin of the reference-loading axes falls outside the $M_x - M_y$ interaction curve, even for cases with irregular structural steel under eccentric compression

- (2) Strain gradient along section should be properly considered in the strain-stress model of confined concrete when conducting the section analysis of hybrid columns under biaxial loading. Use of Lam and Teng's model [5] for confined concrete in section analysis results in an upper limit of load carrying capacity of the hybrid columns under biaxial loading, thus leading to an unsafe prediction, especially for cases with a large eccentricity.
- (3) Quick convergence has been observed in all cases presented, demonstrating the validity and accuracy of the proposed approach for the rapid section analysis and design of FRP-confined concrete-encased arbitrarily shaped steel columns.

Data Availability

The data used to support the findings of this study are available from the corresponding author upon request.

Disclosure

Publication of the present paper has been approved by Professor J.G. Teng at the Hong Kong Polytechnic University, China, who supervised the second author for part of the work in the present paper.

Conflicts of Interest

The authors declare that there are no conflicts of interest regarding the possible publication of the present paper.

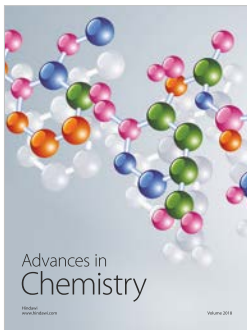
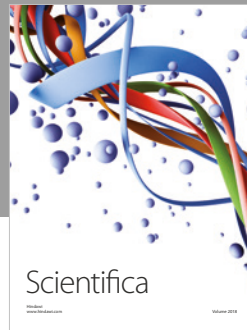
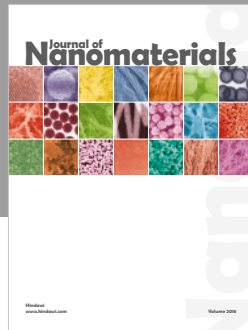
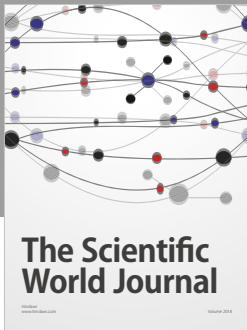
Acknowledgments

The authors are grateful for the financial support received from the Nature Science Foundation of China (Project no. 51608130) and China Postdoctoral Science Foundation (Project no. 2016M602441).

References

- [1] H. Kupfer, H. K. Hilsdorf, and H. Rusch, "Behavior of concrete under biaxial stresses," *ACI Journal Proceedings*, vol. 66, no. 8, pp. 656–666, 1969.
- [2] J. B. Mander, M. J. N. Priestley, and R. Park, "Theoretical stress-strain model for confined concrete," *Journal of Structural Engineering, ASCE*, vol. 114, no. 8, pp. 1804–1826, 1988.
- [3] L. H. Han, W. Li, and R. Bjorhovde, "Developments and advanced applications of concrete-filled steel tubular (CFST) structures: members," *Journal of Constructional Steel Research*, vol. 100, pp. 211–228, 2014.
- [4] K. Karimi, W. W. El-Dakhkhni, and M. J. Tait, "Performance enhancement of steel columns using concrete-filled composite jackets," *Journal of Performance of Constructed Facilities*, vol. 25, no. 3, pp. 189–201, 2011.
- [5] L. Lam and J. G. Teng, "Design-oriented stress-strain model for FRP-confined concrete," *Construction and Building Materials*, vol. 17, no. 6-7, pp. 471–489, 2003.
- [6] M. Samaan, A. Mirmiran, and M. Shahawy, "Model of concrete confined by fiber composites," *Journal of Structural Engineering*, vol. 124, no. 9, pp. 1025–1031, 1998.
- [7] J. G. Teng, T. Yu, Y. L. Wong, and S. L. Dong, "Hybrid FRP-concrete-steel tubular columns: concept and behavior," *Construction and Building Materials*, vol. 21, no. 4, pp. 846–854, 2007.
- [8] O. I. Abdelkarim and M. A. Elgawady, "Analytical and finite-element modeling of FRP-concrete-steel double-skin tubular columns," *Journal of Bridge Engineering*, vol. 20, no. 8, 2015.
- [9] O. I. Abdelkarim and M. A. Elgawady, "Behavior of hollow FRP-concrete-steel columns under static cyclic axial compressive loading," *Engineering Structures*, vol. 123, pp. 77–88, 2016.
- [10] O. I. Abdelkarim, M. A. Elgawady, A. Ghenni, S. Anumolu, and M. Abdulazeez, "Seismic performance of innovative hollow-core FRP-concrete-steel bridge columns," *Journal of Bridge Engineering*, vol. 22, no. 2, 2017.
- [11] T. Ozbakkaloglu and Y. Idris, "Seismic behavior of FRP-high-strength concrete-steel double-skin tubular columns," *Journal of Structural Engineering*, vol. 140, no. 6, 2014.
- [12] S. B. Talaeitaba, M. Halabian, and M. Ebrahim Torki, "Nonlinear behavior of FRP-reinforced concrete-filled double-skin tubular columns using finite element analysis," *Thin-Walled Structures*, vol. 95, pp. 389–407, 2015.
- [13] Y. F. Yang and L. H. Han, "Concrete-filled double-skin tubular columns under fire," *Magazine of Concrete Research*, vol. 60, no. 3, pp. 211–222, 2008.
- [14] X. Liu, A. Nanni, and P. F. Silva, "Rehabilitation of compression steel members using FRP pipes filled with non-expansive and expansive light-weight concrete," *Advances in Structural Engineering*, vol. 8, no. 2, pp. 129–142, 2005.
- [15] K. Karimi, M. J. Tait, and W. W. El-Dakhkhni, "Testing and modeling of a novel frp-encased steel-concrete composite column," *Composite Structures*, vol. 93, no. 5, pp. 1463–1473, 2011.
- [16] K. Karimi, M. J. Tait, and W. W. El-Dakhkhni, "Influence of slenderness on the behavior of a FRP-encased steel-concrete composite column," *Journal of Composites for Construction*, vol. 16, no. 1, pp. 100–109, 2012.
- [17] T. Yu, G. Lin, and S. S. Zhang, "Compressive behavior of FRP-confined concrete-encased steel columns," *Composite Structures*, vol. 154, pp. 493–506, 2016.
- [18] L. Huang, T. Yu, S. S. Zhang, and Z. Y. Wang, "FRP-confined concrete-encased cross-shaped steel columns: concept and behaviour," *Engineering Structures*, vol. 152, pp. 348–358, 2017.
- [19] S. F. Chen, J. G. Teng, and S. L. Chan, "Design of biaxially loaded short composite columns of arbitrary section," *Journal of Structural Engineering*, vol. 127, no. 6, pp. 678–685, 2001.
- [20] T. Ozbakkaloglu and J. C. Lim, "Axial compressive behavior of FRP-confined concrete: experimental test database and a new design-oriented model," *Composites Part B: Engineering*, vol. 55, no. 12, pp. 607–634, 2013.
- [21] Y. F. Wu and Y. G. Cao, "Effect of load path on behavior of FRP-confined concrete," *Journal of Composites for Construction*, vol. 21, no. 4, 2017.
- [22] Y. F. Wu and Y. Wei, "General stress-strain model for steel and FRP-confined concrete," *Journal of Composites for Construction*, vol. 19, no. 4, 2015.

- [23] L. Lam and J. G. Teng, "Ultimate condition of fiber reinforced polymer-confined concrete," *Journal of Composites for Construction*, vol. 8, no. 6, pp. 539–548, 2004.
- [24] T. Yu, Y. L. Wong, J. G. Teng, S. L. Dong, and E. S. Lam, "Flexural behavior of hybrid FRP-concrete-steel double-skin tubular members," *Journal of Composites for Construction*, vol. 10, no. 5, pp. 443–452, 2006.



Hindawi
Submit your manuscripts at
www.hindawi.com

